On Reconstructing Surfaces of Arbitrary Topology from a Range Image

MERCEDES GONZALES MÁRQUEZ[1], WU SHIN-TING[1], ROSANA MARQUES DA SILVA[2]

[1]DCA – Faculty of Electrical and Computer Engineering
State University of Campinas, 13081–970 São Paulo, Brazil
{meche,ting}@dca.fee.unicamp.br
[2]Department of Mathematics and Statistics, Center of Science and Technology
Federal University of Paraiba, P B, Brazil 58109-970
rosana@dme.ufpb.br

Abstract. To reconstruct a topologically consistent 3D surface model is a challenging problem. In this paper we present an algorithm that estimates from a range image, without registering and converting it into a volumetric data, the most probable topology of a surface to be reconstructed. In our algorithm we start with a closed initial mesh and preserve its "closeness" during the reconstruction process. Some experiments were carried out to validate our proposal.

1 Introduction

The problem of reconstructing a surface from a set of sample points is required in many applications such as robotics, computer graphics, geometric modeling, and computer vision. In this paper we consider a specific reconstruction problem in which the input is a range image $\mathcal{R}$ acquired from a surface S, and the desired output is a triangular mesh with vertex set belonging to the sampled data $\mathcal{R}$. Furthermore, the resulted triangular mesh has the most probable topology of the surface S.

Based on the dynamic balloon model [2], the *radial flow model* (RFM) [13] is a method for reconstructing from a range image $\mathcal{R}$, e.g. Figure 1.a, a surface with genus zero, (Figure 1.c). It starts with a simple triangular mesh (Figure 1.b) covered by the sampled data $\mathcal{R}$. A radial inflation force on its vertices make them move towards the samples in $\mathcal{R}$. While the mesh inflates, its triangles may be subdivided adaptively, in such a way that a mesh with evenly distributed vertices is ensured. Because that from a growing center solely a star-shaped region of $\mathcal{R}$ is reached, more than one center may be set for correct fitting.

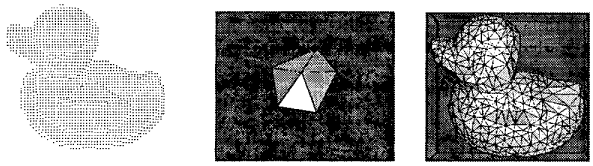

(a) (b) (c)

Figure 1: Radial Flow Model

Da Silva [4] also outlined a way to use RFM for reconstructing surfaces with arbitrary topology. It consists on

1. estimating the topology of S,
2. establishing when the genus of the deforming mesh should be changed, and
3. performing topological surgeries on the deforming mesh.

As far as we know, there are some works addressing dynamic topological updates on the physically-based deforming mesh. They extract surfaces of arbitrary topology from volumetric data [8, 12]. The dynamic evolution for the mesh is governed either by the Euler-Lagrange equation or by global minimization rules. In addition, Curless and Levoy proposed a method for converting range data into a volumetric model to apply this reconstruction technique to range images [3]. The drawback of this reconstruction approach is that it depends strongly on the internal and external forces to be defined *a priori* from the input data and features.

Unlike previous works, RFM is a reconstructing method which does not require to convert a range image into a volumetric representation. Only on the basis of the planar geometry of the range image and range sample points, one can control dynamically the topology of the reconstructed mesh as it inflates towards the sample points. Moreover, following the method proposed by Chen and Medioni [2], we do not need explicitly any internal and external forces for deforming our mesh.

In this work we present an implementation of the ideas presented by Da Silva [4]. We suggest estimating the topology of the surface $\mathcal{S}$ by detecting inner "holes" in its scanned range image $\mathcal{R}$ (regions of pixels with depth equal to zero). To determine the instant that the topology of the reconstructed mesh should be changed for better tailoring

1530-1834/01 $10.00 © 2001 IEEE

the sample points, we propose watching the approaching of two growing fronts that are path-connected by the border of a inner hole. And, finally, a topological surgery consists simply in "cutting" one face from each growing front and "gluing" their borders through a strip of triangular faces.

The remainder of this paper is organized as follows. To be self-contained, we present in Section 2 some concepts and terminology useful for this work. Section 3 describes briefly the steps that are required to fit a set of sample points using RFM, and summarizes the theoretical results concerning topological updates on the reconstructed mesh that Da Silva obtained. Section 4 gives our proposal and Section 5 shows some examples. Finally, in Section 6 some concluding remarks are drawn.

2 Background

Given a surface $\mathcal{S}$ and a direction z, the *height function* in this direction, $f : S \rightarrow R$, is the projection of $\mathcal{S}$ onto the directed line in the direction of z [7].

A *critical point* of a real function f is a point at which the gradient of f vanishes. Critical points are classified by their indices. The index of a critical point p is the number of negative eigenvalues of the Hessian matrix of f at p

$$H(p) = J(\nabla f(p)) = \begin{bmatrix} f_{xx}(p) & f_{xy}(p) \\ f_{yx}(p) & f_{yy}(p) \end{bmatrix}.$$

Hence, the index of a critical point can be 0, 1 or 2, which corresponds, respectively, to a minimum, a saddle point and a maximum. The topology of the level set changes at these critical points. (Figure 2). At a saddle-

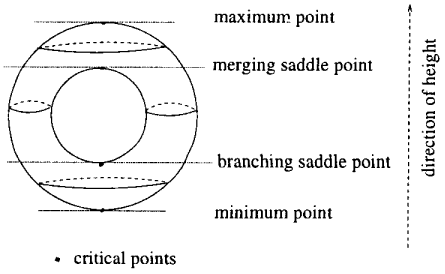

Figure 2: Critical points of a torus.

point either a connected curve may be split into two curves (*branching saddle-point*) or two curves merged in a curve (*merging saddle-point*).

The *Euler characteristic* χ of a surface $\mathcal{S}$ is topologically invariant. The Euler characteristic of a closed and orientable surface of genus g is $2 - 2g$. It can also be expressed in terms of the number of critical points of $\mathcal{S}$

$$2 - 2g = N_{max} + N_{min} - N_{sad} \qquad (1)$$

where N_{max}, N_{min}, and N_{sad} are, respectively, the number of maximums, the number of minimums, and the number of saddles of the surface [10, 9].

Let S_1 and S_2 be two disjoint closed surfaces. Their *connected sum* [9], denoted by $S_1 \# S_2$, is obtained by *cutting* a small circular hole in each surface, and then *gluing* the two surfaces together along the boundaries of the holes. More precisely, we choose subsets $D_1 \subset S_1$ and $D_2 \subset S_2$, such that D_1 and D_2 are closed discs, and define a homeomorphism h of the boundary circle of D_1 onto the boundary of $D2$. Then $S_1 \# S_2$ is obtained by identifying the points x and $h(x)$ for all points x in the boundary of D_1 (Fig. 3).

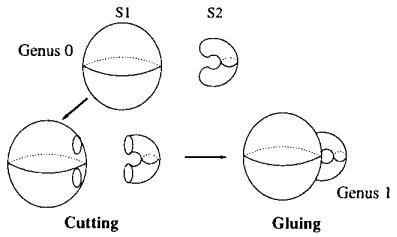

Figure 3: Topological surgery

The connected sum of two disjoint surfaces is also known as *topological surgery*.

3 The Radial Flow Model

In this section the RFM reconstruction procedure and some theoretical foundations developed by Da Silva [4] for applying topological surgeries on the reconstructed model are given. Points in the illustrations correspond to the given range data.

3.1 The Procedure

From the range data $\mathcal{R}$ a convenient initial reference system is determined and a vertex v_0 of an initial closed mesh $\mathcal{M}^0$ (decahedron) is placed on the origin $\mathcal{O}$ of this reference system. From this origin a star-shaped image region is determined. A region $R \subset \mathcal{R}$ is called star-shaped, when a ray from $\mathcal{O}$ to every $p \in R$ only intersects with R in p. As v_0 is fixed during the radial growing process, it is called an *inactive point*. The rest of the vertices builds a *growing front*. $\mathcal{O}$ is indeed the radial center of this growing front. Figure 4.a shows the initialization for the range image given in Figure 4.b. $\mathcal{M}^0$ is covered by the range data and its inactive vertex is the common vertex of its bottom faces.

Next, a radial force is exerted, making the mesh inflate as each of its vertices moves radially towards a *corresponding* (sample) *point* in R. Corresponding points of the vertices of a face $f \in \mathcal{M}^0$ induce a *corresponding region* $r \subset R$ to f.

(a) (b)

Figure 4: (a) Initial $\mathcal{M}^0$ and R concerning the (b) range image $\mathcal{R}$

To adjust a mesh $\mathcal{M}^i$ to a particular detail of the sample points, an edge v_iv_j in the mesh is subdivided if the following conditions are fulfilled:

- its length is greater than a specified tolerance,
- one of their adjacent faces has reconstruction error. The reconstruction error of a face $f \in \mathcal{M}^i$ is determined from the radial distance of f to the points in its corresponding region (Figure 5),

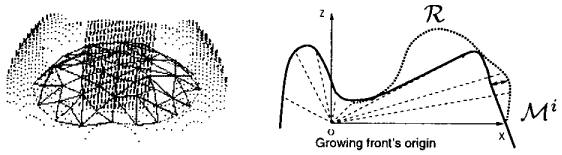

(a) (b)

Figure 5: (a) $\mathcal{M}^i$ in relation to R and (b) its reconstruction error in a 2D view.

- their adjacent faces satisfy the *quality value*

$$||e_{max}|| < 1.25||e||,$$

where $||e_{max}||$ is the length of the greater edge of the face, to avoid the "degenerated" faces, and

- there is a corresponding point in a solid angle defined by the two adjacent faces of v_iv_j (Figure 6).

(a) (b)

Figure 6: (a) Points of R inside of (b) a solid angle

It is worth remarking that, in order to improve the quality of the reconstructed mesh, we keep a Delaunay triangulation whenever a new vertex is inserted in the mesh. The incremental insertion algorithm of Lawson [1] is applied.

The sequence of operations refining–inflating is repeated until no more subdivision and no more inflation is possible, as in the case of *parallel faces*. The parallel faces are the ones whose normal vector is almost orthogonal to the inflating direction (Figure 7).

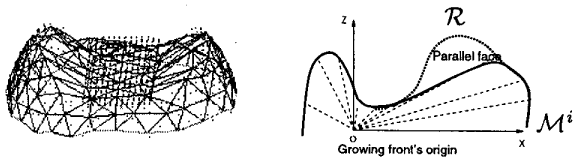

(a) (b)

Figure 7: Parallel faces (a) in $\mathcal{M}^i$ and (b) a 2D view of them.

When no more inflation is possible, reconstruction errors are evaluated. The triangular faces that still have reconstruction errors are grouped into disjoint sets of faces for building new fronts (of growth). From each of them a new radial reference system and new star-shaped corresponding region are determined before carrying out again the cyclic sequence refining–inflating to yield a new mesh $\mathcal{M}^{i+1}$ (Figure 8).

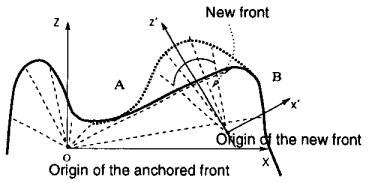

Figure 8: Reference system of a new front in a 2D view.

Whenever a face without reconstruction error is detected, we mark it as an *anchored face*. If there is no face in the mesh $\mathcal{M}^i$ with reconstruction error, it is considered that the aimed reconstructed 3D model is reached. Figure 9

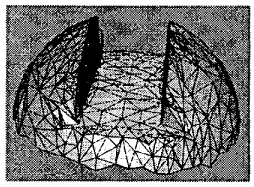

Figure 9: A reconstructed model.

presents a reconstructed triangular mesh from the range image rendered in Figure 4.b.

3.2 Topological Updates

The proof of the propositions and the corollaries given in this section may be found in the doctorate thesis of Da Silva [4].

Proposition 3.1 *Let $\mathcal{M}$ and $\mathcal{R}$ be, respectively, a regular surface and its range image in the direction λ. Let f_h and g_h be the height functions of $\mathcal{M}$ and $\mathcal{R}$, respectively, in the direction perpendicular to λ. $p_{\mathcal{R}}$, with continuous height values in the domain where $\mathcal{M}$ is defined, is a critical point of g_h, if and only if, its correspondence $p_{\mathcal{M}}$ is a critical point of f_h.*

The "continuity" in the height values is required for getting rid of the false critical points as illustrated in Figure 10.

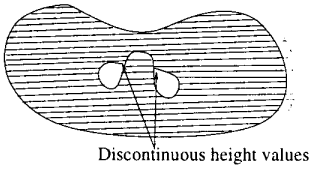

Figure 10: False critical points

Since from one range image it is not possible to infer what is behind the view, we may consider, without loss of generality, that the scanned original surface is C^0-continuous and the unseen part should be somehow "filled". Then, for estimating the genus in $\mathcal{M}$ we may reduce the range image $\mathcal{R}$ into a binary image $\mathcal{I}$ by attributing 0 to the pixel where the depth value is zero, and 1, otherwise.

The following corollary ensures us that the number of critical points in $\mathcal{M}$ cannot be less than the number of critical points in $\mathcal{I}$.

Corollary 3.1 *Let f_h and g_h be the height functions of $\mathcal{M}$ and $\mathcal{I}$, respectively. If $p_{\mathcal{I}}$ is a critical point of g_h, then its correspondence $p_{\mathcal{M}}$ is a critical point of f_h.*

We may have more than one critical point along the direction λ (hidden critical points). The following corollary gives us the lowerbound of the genus in $\mathcal{M}$.

Corollary 3.2 *The genus in $\mathcal{I}$ is less or equal than the genus in $\mathcal{M}$.*

Consequently, topological surgeries on the reconstructed mesh $\mathcal{M}^i$ are necessary whenever the number of holes in $\mathcal{I}$ is greater than the genus of $\mathcal{M}^i$.

Now, the following corollary tells us the instant that a topological surgery should be performed.

Corollary 3.3 *Let $\mathcal{A}_1, \mathcal{A}_2 \subset \mathcal{M}^k$ be two distinguishing maximally connected unanchored face sets and $\mathcal{I}_1$ and $\mathcal{I}_2 \subset \mathcal{I}$ be, respectively, the corresponding regions. If at iteration j the corresponding regions of $\mathcal{A}_1$ and $\mathcal{A}_2$ become adjacent, then there is a height function of $\mathcal{I}$ for which there is a merging saddle-point in the neighborhood of $\mathcal{I}_1$ and $\mathcal{I}_2$.*

And, finally, there are two propositions that show us how to change the genus and to maintain the orientation of the reconstructed mesh, respectively.

Proposition 3.2 *The merge of two sets of maximally connected unanchored faces belonging to a closed surface increments the genus by 1.*

Proposition 3.3 *The orientation of $\mathcal{M}$ is preserved by topological surgery (Figure 11).*

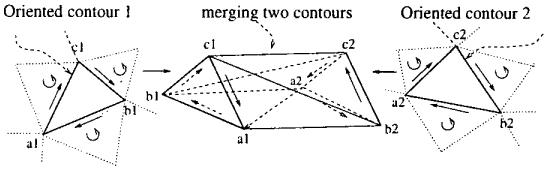

Figure 11: Merging.

4 Our Proposal

As already explained in Section 3.2, we consider that $\mathcal{M}$ is C^0-continuous and, instead of $\mathcal{R}$, we may use the binary image $\mathcal{I}$ for inferring the topological properties of the model $\mathcal{M}$ to be reconstructed.

To implement the theoretical foundations presented in Section 3.2 we should devise procedures for

- segmenting $\mathcal{I}$ by detecting its inner and outer borders,
- segmenting the given range image $\mathcal{R}$ by partitioning it into a set of star-shaped subregions,
- detecting when a topological surgery is necessary, and
- performing a topological surgery.

These procedures were developed separately and integrated into the previous version of the RFM.

4.1 Border Detection

There is a variety of work focusing on the border detection [5]. Our task was restricted on testing some of them for accomplishing our goal which is to get accurately the connected components and their oriented borders in the corresponding binary image $\mathcal{I}$ of the given range image $\mathcal{R}$.

For obtaining the oriented border from a range image, we chose the Chain-Code algorithm [5]. This technique is based on 8-connectivity. We start with a point and walk on the black or white connected region boundary, looking for the border points. In our preliminary tests we realized that two kinds of noises occur frequently and the algorithm failed. They are the salt and pepper noises (Figure 12).

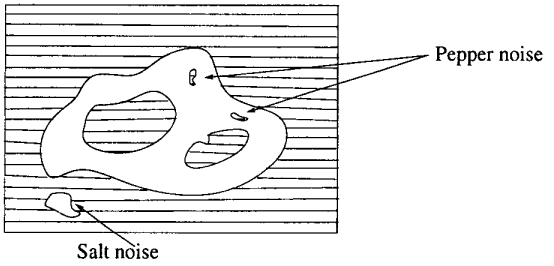

Figure 12: Salt and pepper noises.

Then, before applying the Chain-Code algorithm, we segment the binary image $\mathcal{I}$ into maximally connected regions containing pixels with value 1 (white regions), determine their areas, and remove all of "isolated" regions containing pixels with value 0 whose area is less than a predefined threshold (pepper noises), by attributing value 1 to their pixels. Following, we re-segment the binary image $\mathcal{I}$ into maximally connected regions containing pixels with value 0 (black regions), and remove analogously all of "isolated" white regions (salt noises), by attributing value 0 to their pixels.

This preprocessing, besides allowing us to apply the Chain-Code technique, gives us an estimation of the genus that the model $\mathcal{M}$ may have. According to the Corollary 3.2 the number of bounded black regions cannot be greater than the genus in $\mathcal{M}$. Moreover, it delivers us the allowable region (white one) for placing the initial mesh.

4.2 Determination of Star-Shaped Regions

From Proposition 3.1, if a closed surface has genus 0 then the corresponding binary image $\mathcal{I}$ of its range image $\mathcal{R}$ is simply connected. The previous implementation of RFM only considered that the planar geometry of $\mathcal{I}$ is a star-shaped one, which is simply connected. Hence, it has worked well for reconstructing most surfaces with genus 0. For each object, only one *inactive vertex* is necessary and, on the demand, the radial center is translated in the space for creating new growing fronts in order to reach every 3D sample point. Each radial center was defined as follows. It is computed a line that passes by the barycenter of a potential growing front and has the direction of the approximate "normal vector" of its contour. The radial center is a point on this line, such that the front contour lies within a solid angle of 45° defined by this point (Figure 8) [13].

Corollary 3.2 tells us that if $\mathcal{I}$ is multiply connected, then the model $\mathcal{M}$ to be reconstructed has genus greater than zero. With one *inactive vertex* one cannot reach completely the border of $\mathcal{I}$ without overlapping or "filling" the holes. Hence, we suggest partitioning $\mathcal{I}$ into several star-shaped regions, each of them is covered unambiguously by a radial center (Figure 13).

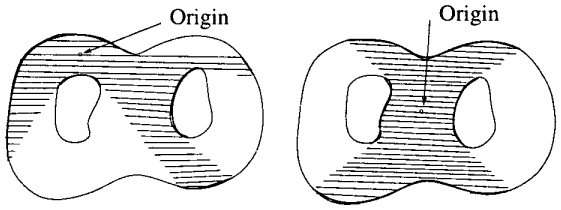

Figure 13: Unambiguous coverage of a radial center in multiply connected images.

The parallel faces that are adjacent to the base of the maximal coverage of a radial center are called *limit border faces* (Figure 14).

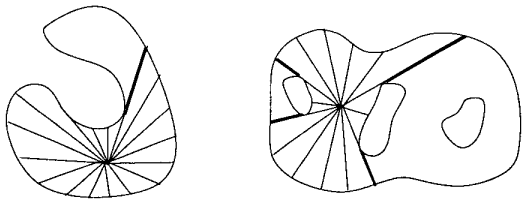

Figure 14: (a) One (b) Four limit border faces.

For each radial center on $\mathcal{I}$ a new *inactive vertex* is inserted. Emulating the fluid flow, we place a new *inactive vertex* on the midpoint of the base-edge of the *limit border face* and set the radial center on the line that intersects this midpoint and that is parallel to the height direction of the given range image. In this way, we believe that the mesh is pushed uniformly to most sample points belonging to a growing front (Figure 15).

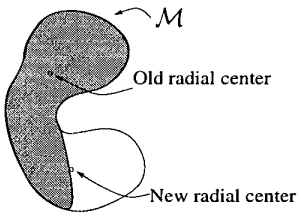

Figure 15: Radial centers in a 2D View

4.3 Conditions for a Topological Surgery

From Corollary 3.3 we know that when two distinguishing growing fronts become very close, there must be a merging saddle-point in the model $\mathcal{M}$. Our challenge was to devise a way for deciding

1. which pair among a set of potential growing fronts, such as shown in Figure 14.b, should be merged, and

2. when they should be merged.

The pair of distinguishing growing fronts that must be glued always share the same inner border. Hence, from one *limit border face* of a growing front we may get its pair by running along the inner border of the image $\mathcal{I}$.

Whenever the scalar product of the normalized normal vectors of their *limit border faces* is smaller than $(-1+\epsilon)$ and the two segments defined by the border vertices are inside the range image, we consider that they are close enough for surgery. These two conditions are regarded as *proximity criteria* for a topological surgery.

4.4 Topological Surgery

Analogous to the procedure depicted in Figure 11, it comprises two stages (Figure 16):

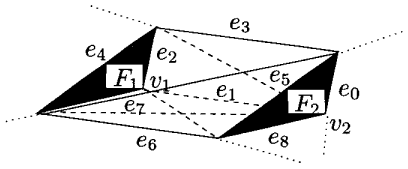

Figure 16: Cutting and gluing.

1. Cutting : the *limit border faces* F_1 and F_2 of the two fronts are removed.

2. Gluing : to preserve the orientability of the mesh $\mathcal{M}$, we first insert the edge e_1 to connect the two base vertices v_1 and v_2 on the inner border. Then, we create a face f_1 by closing the sequence $e_0e_1e_2$ with the edge e_3, and a face f_2 by closing the sequence $e_5e_3e_4$ with the edge e_6. Finally, we close the mesh with a face f_3. A triangulation is performed on these three faces along their diagonal.

After each topological surgery we merge two growing fronts into one. The radial center of this new growing front is placed on the line that passes by the midpoint of the common edge of the two new (base) faces derived from f_3 and that is parallel to the height direction of $\mathcal{R}$. This placement favors the upwards growing.

5 Experimental Results

We have implemented our procedures in C on a SUN-SPARC platform and integrated into the previous version of RFM.

To show how our algorithm works, let us present the reconstruction of a torus (Figure 17.b) from the synthetic

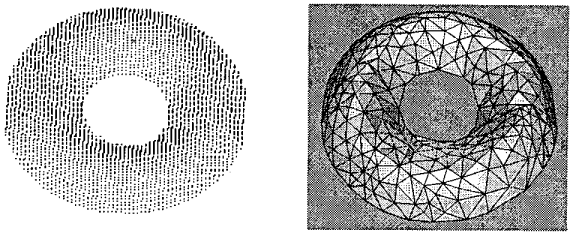

(a) (b)

Figure 17: (a) A rendered range image and (b) reconstructed mesh.

range image $\mathcal{R}$ of 128 × 128 (9915 points) shown in Figure 17.a. The initial mesh is a decahedron (Figure 18.a) and the radial center covers partially $\mathcal{R}$. The mesh grows until it reaches the limit of the maximal coverage (Figure 18.b). Observe that two *limit border faces* resulted, each in one "extreme" of the mesh. These faces are indeed parallel faces. A new radial center and a new coverage are, then, determined and the mesh grows further under the new radial inflation force (Figure 18.c) until the growing possibilities are exhausted (Figure 18.d). Again, a new radial center and a new coverage are computed and the mesh is further inflated (Figure 18.e). When the proximity criteria are satisfied (Figure 18.f), a topological surgery is performed (Figure 18.g), and a new radial center is evaluated. With upwards inflating force, the rest of faces are pushed to the sample data (Figure 18.h).

We also selected some results we obtained with synthetic images and a real range image. Reconstructed meshes have been rendered in GeomView [6].

We tested our algorithm on a synthetic range image of a tritorus of size 255×123 (22312 points). Three views are presented in Figure 19: input data, a front and a back view of the corresponding reconstructed mesh. In this case, we observed that our algorithm can match correctly pairs of growing fronts and perform three topological surgeries.

We also reconstructed a mesh from a synthetic range image 123 ×189 (16071 points) which contains depth discontinuity (Figure 20). Since in our procedure we take the assumption that the original surface is C^0-continuous, when ambiguous interpretation arises, the upper and the lower border on the discontinuity are automatically connected. As a result, the genus in the reconstructed model is always equal to the genus in the given range image.

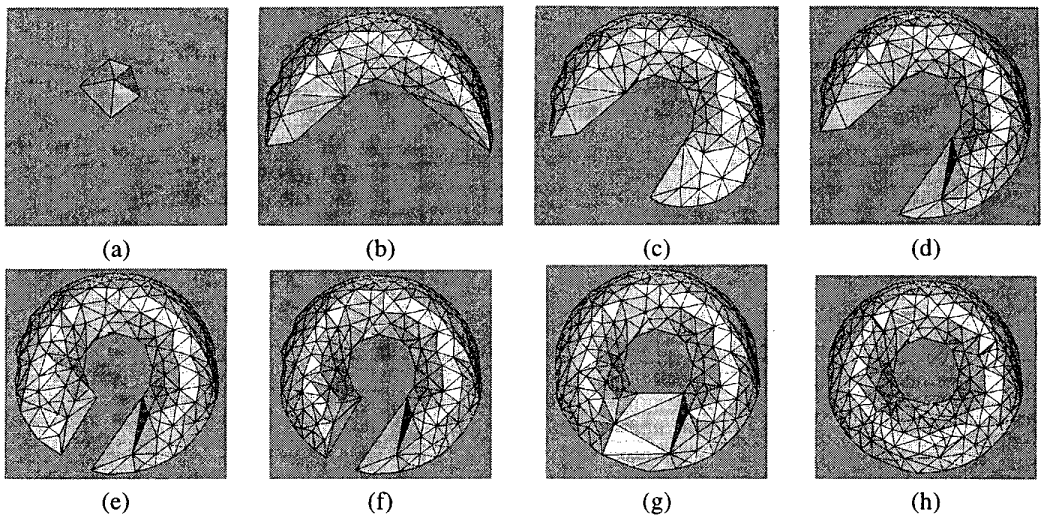

Figure 18: A reconstruction sequence.

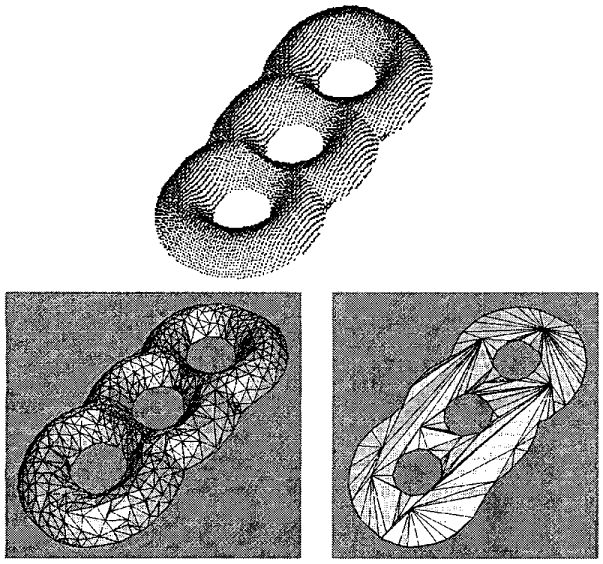

Figure 19: Tritorus.

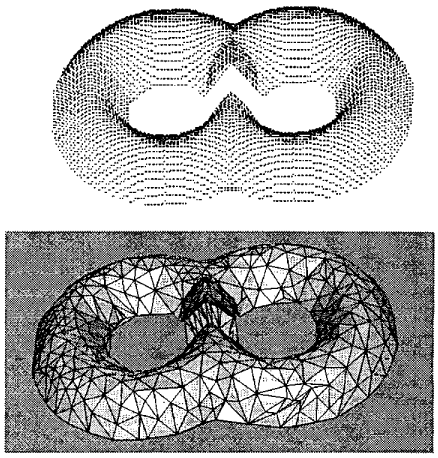

Figure 20: Bitorus.

Finally, we present two reconstructed meshes from a real range image of 200×240 (14127 points) taken from database available in the internet [11]. Note that in this image we have a hard border. Independent of the pre-defined tolerance, the topology of the reconstructed model is the same. The tolerance only affects the mesh refinement (Figure 21).

6 Conclusions

We have presented an extension to RFM algorithm in order to support the reconstruction of arbitrary topological classes of objects from a range image.

Our algorithm can automatically infer the topological class of a surface to be reconstructed from the given range image. Moreover, necessary topological updates on the mesh can be dynamically detected and performed while it grows, until it adjusts to the sample data in a pre-defined tolerance.

We observed that our extension also improves the reconstruction of a surface homeomorphic to a sphere, when the binary image $\mathcal{I}$ of their range image $\mathcal{R}$ is not star-shaped

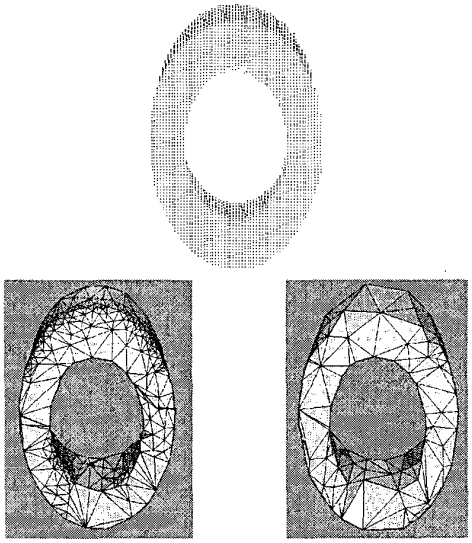

(a) τ = 1.5 units for error (b) τ = 4.5 units for error

Figure 21: Taperoll.

as illustrated in Figure 22.

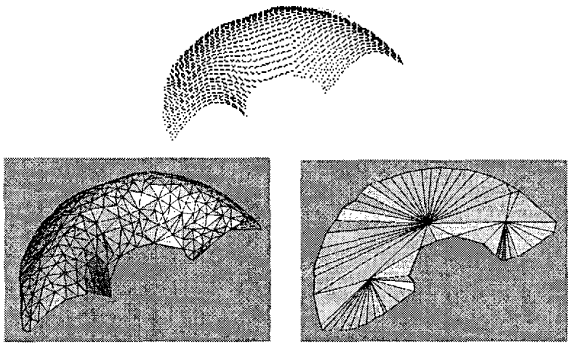

Figure 22: An image with non-star-shaped border

As further work, we intend to provide a mechanism that integrates incremental- and dynamically the range images from different views to reconstruct completely a 3D closed surface model.

Acknowledgement

This work is partially supported by FAPESP under the Grant No 00/10913-3.

References

[1] M. Berg and et.al. *Computational Geometry: Algorithms and Applications*. Springer-Verlag, 2 edition, 2000.

[2] Y. Chen and G. Medioni. Description of complex objects from multiple range images using an inflating balloon model. *Computer Vision and Image Understanding*, 61, pp. 325-334(3), 1995.

[3] Brian Curless and Marc Levoy. A volumetric method for building complex models from range images. In *Computer Graphics Proceedings*, pages 303–312, New Orleans, August 1996. SIGGRAPH 96.

[4] R.M. da Silva. *Reconstruction of a 3D Model from Range Images by Using Deformable Models*. PhD thesis, State University of Campinas, Campinas, São Paulo, Brazil, December 1999. (In Portuguese).

[5] R.C.Gonzalez e R.E.Woods. *Digital Image Processing*. Addison-Wesley, 1992.

[6] Geomview. http://www.geom.umn.edu/software/download/geomview.html.

[7] J.C. Hart. Morse theory for computer graphics. Technical Report EECS-97-002, Washington State University, 1997.

[8] A. Montanvert J.-O. Lachaud. Deformable meshes with automated topology changes for coarse-to-fine three-dimensional surface extraction. *Medical Image Analysis*, 3(2):187–207, 1998.

[9] W.S. Massey. *Algebraic Topology - An Introduction*. Springer - Verlag, Ney York, 1967.

[10] J. Milnor. *Annals of Mathematics Studies: Morse Theory*, volume 51. Princeton University Press, 1963.

[11] Isolated range images. http://sampl.eng.ohio-state.edu/sampl/data/3DDB/RID/MSU/Isolated.

[12] D. Terzopoulos T. McInerney. Topology adaptive deformable surfaces for medical imaging volume segmentation. *IEEE Transactions on Medical Imaging*, 18(10):840–850, 1999.

[13] S.-T. Wu, R.M. da Silva, and M.R.G. Márquez. Reconstructing a 3d model from an unregistered range image. In *Proceedings of the International Conference on Imaging Science, Systems and Technology*, volume 1, pages 297–303, Las Vegas, Nevada, USA, June 2000.